Desalination and Water Treatment
www.deswater.com

doi: 10.5004/dwt.2017.20555

71 (2017) 302–311
April

High performance in power generation by pressure-retarded osmosis (PRO) from hypersalinity gradient: case study of hypersaline Lake of Urmia, Iran

Hamidreza Sharifan[a,c,*], Henrik T. Madsen[b], Audra Morse[a]

[a]*Department of Civil, Environmental, and Construction Engineering, Texas Tech University, Office # 018, Lubbock, TX 79409–1023, USA, Tel. +1-806-834-3783; emails: hsharifan@tamu.edu, hsharifan@gmail.com (H. Sharifan), Tel. +1-806-742-3451; email: audra.n.morse@ttu.edu (A. Morse)*
[b]*Department of Chemistry and Bioscience, Aalborg University, A.C Meyers Vænge, 2450 Copenhagen, Denmark, email: htm@bio.aau.dk*
[c]*Zachry Department of Civil Engineering, Texas A&M University, TAMU 3136, College Station, TX 77843-3136, USA*

Received 30 October 2016; Accepted 24 January 2017

ABSTRACT

Pressure-retarded osmosis (PRO) is a renewable energy that generates its energy from mixing freshwater streams with saline water. The limitation of this energy has been reported to be 0.192 kWh/m^3 of the mixed solution when using seawater as the saline source, which could limit the potential of the technology. However, using hypersaline water sources allows for higher energy densities, and could be a way to make PRO viable. Lake Urmia in Iran is the second largest hypersaline lake in the world, and in this study, the PRO potential has been evaluated. An energy potential between 250 and 1,250 MW depending on the freshwater source was calculated by using a newly developed mixing model. The results of a new model were compared with previously reported energy potentials of Lake Urmia calculated with simplified models. Based on our analysis the Madsen's model predicts approximately two times higher energy production over these models, showing that a hypersaline PRO plant at Lake Urmia could be a significant producer of renewable energy in the region. Finally, the sensitivity analysis for membrane revenue based on the fluctuation of the retail price of electricity has been carried out. The results of this investigation can be used as a reference to predict energy production from the other hypersaline lakes around the world.

Keywords: Urmia Lake; Pressure-retarded osmosis; Renewable energy; Hypersaline

1. Introduction

In the context of mitigating the effects of climate change, reduction of greenhouse gas (GHG) emissions is the main objective of global climate policy. Sustainable renewable energy is a key approach in achieving this goal [1]. Among sustainable energy sources, pressure-retarded osmosis (PRO) is a promising technology [1–4]. The PRO generates energy from the natural phenomenon of discharging a fresh river water to the saline reservoirs, therefore, the PRO has very low ecological impacts [5,6].

PRO is an emerging membrane separations technology, which can produce renewable energy [7,8]. PRO extracts the Gibbs free energy of mixing by taking advantage of the osmotic flow through a semipermeable membrane from fresh river water to saline water against a hydraulic pressure [9–12]. It has been estimated that the saline gradient energy (SGE) from rivers discharging to oceans could potentially generate 2.6 TW worldwide; this number can cover approximately 20% of the current world energy demand [13]. However, recent studies show that this mixing scheme is limited to a power generation

* Corresponding author.

only up to 0.192 kWh/m^3 of the mixed solution, which leaves little energy for pretreatment and process inefficiencies [11]. To increase the energy density, the use of water from hypersaline lakes has been suggested for investigation [11,14,15].

Lake Urmia in Iran is the second largest hypersaline lake in the world with a considerable number of low salinity rivers discharging into the lake [15–18]. ZarrinehRud River is the major conjugated river of the lake with 43% of the water feed [15]. Lake Urmia has the most optimized geographical location for PRO development in Iran [16,19] and could potentially supply the region with renewable energy.

Previously, two studies have reported on the PRO potential for Lake Urmia. A scientific paper by Emdadi et al. [15], who investigated the potential of placing a PRO plant at the mouth of the ZarrinehRud River and a white paper by Kelada [20], who reported on the potential of using water from the ZarrinehRud River and the Caspian Sea. However, the accuracy of both studies can be questioned. In the study of Emdadi et al. [15], an equation by Forgacs's dating back to at least 1982 was used [21] (see Eq. (1)) and in the estimate made by Kelada [20] the osmotic pressure determined via the Van't Hoff equation was used, which is only strictly valid for low saline solutions. The equation of Forgacs is also founded on the Van't Hoff equation for osmotic pressure:

$$U = Q \times 2RT\left(C_D \ln\frac{2C_D}{C_D + C_C} + C_C \ln\frac{2C_C}{C_D + C_C}\right) \tag{1}$$

where Q is the flow rate of river water into the saline water reservoir, R is the gas constant, T is the absolute temperature, C_D the concentration of the river water and C_C the concentration of the saline water.

Recently, a method for accurately determining mixing energy for hypersaline (NaCl) solutions has been developed by Madsen et al. [11]. This model is based on the use of Pitzer equations, which offer an improved description of solutions of high ionic activity such as hypersaline water [22,23]. In this study, the model was applied to estimate the power potential from mixing of the ZarrinehRud River, and the Caspian Sea with Lake Urmia and the results were compared with those reported by Emdadi et al. and Kelada [15,20].

2. Energy sources

2.1. Lake Urmia

Urmia Lake is the second largest hypersaline lake in the world, and it is located in northwest Iran (North: 36° 45′ to 38° 20′ and East: 44° 50′ to 46° 10′) [24,25] (Fig. 1). It was registered as a Biosphere Reserve by UNESCO and listed as a wetland of international importance under the 1971 Ramsar Convention [24,26,27]. The surface area of the lake has been dramatically reduced during the last decade to 3,100 km^2 as reported in 2009 [15]. The length from north to south varies between 140 and 144 km, and the width is between 16 and 63 km, which covers approximately 3.2% of the entire

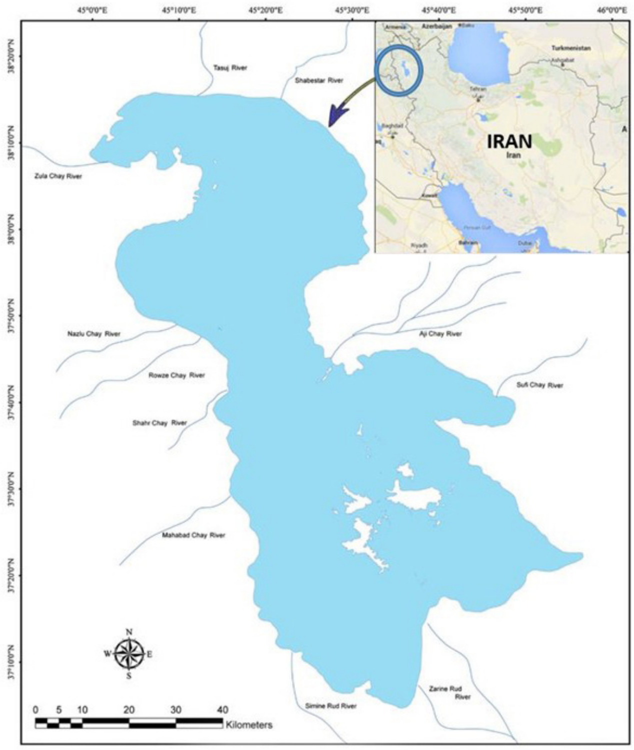

Fig. 1. Geographical location on the Urmia Lake is shown in the blue circle (Karbassi et al. [17]).

Table 1
Characteristics of the rivers discharging to Lake Urmia

River name	Feeding (%)	Length (km)	Main average (m^3/s)	Flow catchmen area (km^2)
ZarinehRud	42	230	45.8	11,897
SiminehRud	13	145	9.5	3,656
Godarchay	10	100	0.34	2,123
Barandoozchay	7	70	8.3	1,318
Nazloochay	7	85	7.87	2,267
Mahabad chay	7	80	6.5	1,528
Shahrichay	4	70	5.33	720
Zoolachay	2	84	–	2,090
Rowzehchay	1	50	1.33	453

country [28], and about 7% of the total surface water of the country [15,18]. The maximum depth of the lake is 16 m [15,18]. The catchment area of the lake receives 21 permanent and 39 seasonal rivers [18]. The main freshwater streams are listed in Table 1 according to feeding percentage [15,29,30]. The Aji Chay River is a saline river discharging to the lake [15,30]. The salinity of Urmia Lake has fluctuated over time 217–340 g/L [14,17].

In the last three decades, the average annual precipitation rate on the lake was reported approximately 342 mm [15,30] and annual evaporation rate was 1,435 mm [30]. If the annual rivers flow adds 1,093 mm water to the lake, water input and output would be balanced with slight change [30]. For example, it was estimated, if 4,351,968,000 m^3 of water annually discharged the Lake through the rivers, the water level of the Lake will rise by 0.978 m and decreased by 0.32 m annually due to evaporation [25,30].

This lake resembles the Great Salt Lake in the Western USA in many morphological, chemical and sediment characteristics [18,30]. The dissolved salts in Lake Urmia decrease the free energy of the water molecules, leading to a drop in the vapor pressure above the lake. Consequently, it lowers the evaporation rate from such lakes compared with freshwater lakes with the same conditions regardless of salinity. Table 2 shows the hydrochemical characteristics of the Urmia Lake, ZarrinehRud River and the Caspian Sea. Since the primary compound in forming the salinity of the Urmia Lake was a high concentration of the NaCl (halite), all calculations in this study were based on the concentration of NaCl in the Lake.

2.2. ZarrinehRud River

ZarrinehRud River is the major river that discharges to Lake Urmia and the average annual flow is about 1,583 million m^3 [15]. It is a long river with a length of approximately 302 km. The amount of total dissolved solids (TDS) of the river has been reported to be <0.1% [15]. Table 2 presents the water quality of the river based on the reported data from the available literature.

2.3. Caspian Sea

In recent years, transferring the water from the Caspian Sea to the Urmia Lake has been considered as a possible solution to restore the Urmia Lake [27,31,32]. However, there is still environmental concerns for this proposed project. The transferring path has been estimated to be approximately 300 km, which may cost 4–5.5 billion USD in a time frame of 5 years' construction [27]. The assessment of this project is one the priority projects approved by the committee to save Lake Urmia under UNDP supervision [31]. This project has the potential for a PRO energy extraction scheme [14], which has not been seriously studied.

3. General mixing theory

The energy potential of hypersaline PRO schemes can be determined by calculating the free energy of mixing [36]. The Gibbs free energy of mixing A and B solutions yields to a mixture (index-M) is presented by Eq. (2).

$$-\Delta G_{mix} = RT\left(\left[\sum x_i \ln\left(\gamma_i x_i\right)\right]_M - \phi_A\left[\sum x_i \ln\left(\gamma_i x_i\right)\right]_A - \phi_B\left[\sum x_i \ln\left(\gamma_i x_i\right)\right]_B\right) \tag{2}$$

In Eq. (2), x_i is the mole fraction, γ_i represents the activity coefficients of each of the species present in the solution and φ_A and φ_B are the mole ratios in solution A and B, respectively, to the total moles in the system ($\varphi_A + \varphi_B = 1$). R is the gas constant and T is the absolute temperature in Kelvin. If solutions A and B contain only water and salt (NaCl) and $\varphi = \varphi_A$, then Eq. (2) may be rewritten as:

$$\begin{aligned}\frac{-\Delta G_{mix}}{RT} &= x_{w,M}\ln\left(\gamma_{w,M}x_{W,M}\right) \\ &\quad + v.x_{s,M}\ln\left(\gamma_{s,M}x_{s,M}\right) - \phi\left(x_{w,A}\ln\left(\gamma_{w,A}x_{W,A}\right) + v.x_{s,A}\ln\left(\gamma_{s,A}x_{s,A}\right)\right) \\ &\quad - \left(1-\phi\right)\left(x_{w,B}\ln\left(\gamma_{w,B}x_{W,B}\right) + v.x_{s,B}\ln\left(\gamma_{s,B}x_{s,B}\right)\right)\end{aligned} \tag{3}$$

In Eq. (3), ν is the dissociation constant of the salt (2 for NaCl). The subscripts w and s refer to water and salt, respectively. This equation is not easily applicable, but by rewriting it into a mass-based model it can be applied to determine the mixing energy of any salt concentration without using any of the approximations that have been used in previous mixing energy models (model by Yip and Elimelech [12]). In most recent models, applicable for hypersaline lakes [11], the generation of energy in the concept of mixing theory was expressed based on mass, m (kg), molal concentrations, m_o (mol/kg solvent) and mass based molar concentrations,

Table 2
Selected water quality characteristic of Lake Urmia and ZarrinehRud River/Caspian Sea [17]

Urmia Lake					ZarrinehRud River					Caspian Sea[b]				
Cations	Conc. (g/L)	Anions	Conc. (g/L)	TDS[a] (g/L)	Cations	Conc. (g/L)	Anions	Conc. (g/L)	TDS[a] (g/L)	Cations	Conc. (g/L)	Anions	Conc. (g/L)	TDS[a] (g/L)
Na^+	125	Cl^-	216	324	Na^+	0.01	Cl^-	0.0072	0.289	Na^+	3.6	Cl^-	6.1	1.42
Mg^{2+}	11.3	SO_4^{2-}	22.4		Mg^{2+}	0.009	SO_4^{2-}	0		Mg^{2+}	2	SO_4^{2-}	6.1	
K^+	2.63	HCO_3^-	1.38		K^+	0.001	HCO_3^-	0.176		K^+		HCO_3^-	0.2	
Ca^{2+}	0.55				Ca^{2+}	0.042				Ca^{2+}	3.3			

[a]The amount of TDS for Lake Urmia was reported from Ahmadzadeh Kokya et al. [25], ZarinnehRud River from Kelts and Shahrabi [33] and Caspian Sea from Pervov et al. [34].
[b]The water quality concentration from the Caspian Sea was extrapolated from Ghadiri et al. [35].

C_m (mol/kg solution). Therefore, Eq. (3) by substituting mass instead of volume can be rewritten as:

$$\frac{-\Delta G_{mix}}{RT} = \frac{C_{m,w,M}}{\phi_m}\ln\left(\gamma_{w,M}x_{w,M}\right) + \frac{v.C_{m,w,M}}{\phi_m}\ln\left(\gamma_{s,M}x_{s,M}\right) - C_{m,w,A}\ln\left(\gamma_{w,A}x_{w,A}\right) - C_{m,s,A}\ln\left(\gamma_{s,A}x_{s,A}\right) - \frac{1-\phi_m}{\phi_m}C_{m,w,B}\ln\left(\gamma_{s,B}x_{s,B}\right) - \frac{1-\phi_m}{\phi_m}v.C_{m,s,B}\ln\left(\gamma_{s,B}x_{s,B}\right) \quad (4)$$

where φ_m is presenting the mass ratio as it is shown in Eq. (4).

$$\phi_m = \frac{m_A}{m_M}$$

Due to the high ionic strength of hypersaline waters, it is necessary to use an activity model to determine the activity coefficients [11]. In this study, we used the molal-based Pitzer equations for single salt solutions [37,38]. Eq. (5) represents the activity coefficient of the present ionic species as following:

$$\log\left(\gamma\pm\right) = -\left|Z_M Z_X\right| A_\varphi\left[\frac{\sqrt{I}}{1+b\sqrt{I}} + \frac{2}{b}\ln\left(1+b\sqrt{I}\right)\right] + mo_s.\frac{2V_M V_X}{V}\left\{2\beta^0_{MX} + 2\frac{\beta^1_{MX}}{\alpha^2 I}\left[1-\left(1+\alpha\sqrt{I}-\frac{\alpha^2 I}{2}\right)e^{-\alpha\sqrt{I}}\right]\right\} + \frac{3}{2}mo_s^2\left[\frac{2\left(V_M V_X\right)^{\frac{3}{2}}}{V}C^\varphi_{MX}\right] \quad (5)$$

where the subscript MX refers to an ion pair of cation M and anion X. Z_M and Z_X are the charge, and ν_M and ν_X are the number of the cation and anion. A_ϕ is the Debye–Hückel slope for the osmotic coefficient, I is the ionic strength, and β^0, β^1 and C^φ are temperature and pressure dependent constants for the specific ion pair MX. Finally, mo_s is the molal concentration of the salt and b and α are parameters that have values of 1.2 and 2.0 $kg^{1/2}/mol^{1/2}$ for all 1–1, 2–1 and 3–1 ion pairs.

The sign of ± indicates that it represents the activity coefficient of the ion pair, not the individual ions.

3.1. Potential for energy production at the Urmia Lake–ZarrinehRud River system

The results in Table 3 show the potential energy production from the mixing of the ZarrinehRud River with the Urmia Lake. The maximum energy potential from mixing freshwater of the ZarrinehRud River with the hypersaline water of Lake Urmia ranges up to 37.5 MJ/m^3 freshwater at 25°C (10.4 kWh/m^3), significantly higher energy estimate than what was predicted in the study by Emdadi et al. [15]. The reason for higher energy yield is that the model of Forgacs underestimates the free energy of mixing as can be seen in the comparison of the two models in Fig. 2. It can also be seen that the model of Forgacs becomes increasingly inaccurate as the salinity of the lake increases, which leads to a significant underestimation of the energy potential from hypersaline lakes.

The average energy of the mixing of the ZarrinehRud River and Lake Urmia was estimated to be 25.2 MJ/m^3 (7 kWh/m^3) at 25°C, which may apply as a reference quantity production for the efficiency of the other hypersaline reservoirs which may have similar chemical characteristics.

Due to limited freshwater resources, which may impact the power production [39], it is worth considering how much

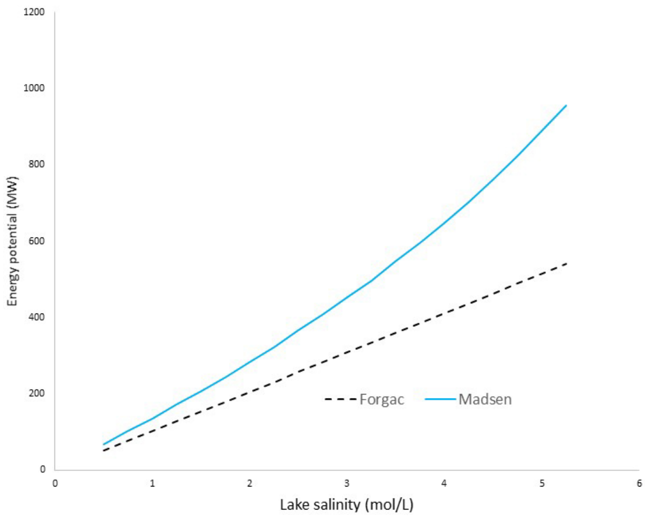

Fig. 2. A comparison of mixing energy potential of Urmia Lake between two presented models of Madsen et al. [11] and Forgacs [21].

Table 3
Estimated technical potential of energy production of ZarrinehRud River at Lake Urmia based on PRO model of Madsen

Year	River discharge (m^3/s)	Lake salinity (mol/L)	NaCl (wt%)	Osmotic pressure (bar)	River salinity (mmol/L)	kWh/m^3 river	Theoretical potential (MW)	Technical potential (MW)	
								Lower limit	Upper limit
1994	33.5	1.69	9.3	86.7	0.48	2.19	264	106	132
1995	34.8	2.84	15	163	0.58	3.92	491	196	246
2000	23	5.2	25.5	393	0.4	8.72	722	289	361
2001	70	5	24.7	370	0.48	8.25	2,079	832	1040
2003	24	4.96	24.5	364	0.44	8.13	702	281	351
2008	33.5	5.82	28.1	478	0.83	10.42	1,257	503	628

alternative freshwater rivers can contribute to producing energy from the Lake Urmia. These freshwater rivers with their physiochemical characteristics are shown in Table 4.

3.2. Potential for energy production at the Urmia Lake–Caspian Sea

Due to the feasibility of transferring water from the Caspian Sea to recover the water loss of Urmia Lake, the energy potential of mixing water from the Caspian Sea with Lake Urmia water was calculated. In a previous study reported by Kelada [20], the potential power of the combining both SiminehRud and ZarinehRud Rivers were estimated 800 MW, while a channel from the Caspian Sea could produce 600 MW giving a total of 1,400 MW [20].

To compare the results of Kelada [20] with those obtained with the new model, the technical potential (MW) for ZarrinehRud River and the Caspian Sea were calculated based on the data and mixing ratios used by Kelada's report [20]. Kelada [20] specified flow rates of ZarrinehRud River and Caspian Sea water of 75 and 100 m^3/s, respectively, mixing 1 m^3 of Urmia water with 3 m^3 freshwater. This is equal to mass ratio ($\varphi_m = 0.71$), and different from the Emdadi et al. study [15] in which a mixing ratio of approximating zero was used. Kelada [20] used a salinity concentration of 320 g/L equal to 26.6 wt%. Using these input data in this study, a theoretical energy potential of 1,053 and 1,134 MW, respectively, for ZarrinehRud River and Caspian Sea were calculated showing a significantly higher energy potential than what was estimated by Kelada [20]. However, as previously argued only a part of this energy can be harvested. Because in practice, technical harvested energy is lower than theoretically estimated energy generation. This difference can be explained by fluctuation in operating pressure, environmental impacts and mass transfer limitations [12,15,41]. In this study, the limits for theoretical potential have been determined by the same approach used by Emdadi et al. [15], where the lower limit represents 40% and the upper limit 50% of the theoretical potential, which are the typical limits used in PRO literature [12,14,42]. Therefore, to harvest the net extractable work in nature the limitation of theoretical energy has to be incorporated into the energy analysis (Table 5). Furthermore, for the scenario of transferring water from the Caspian Sea, it will be necessary to invest energy required for pumping water from the Caspian Sea to Lake Urmia. This was estimated by Kelada [20], to be 300 MW, which must be subtracted from the theoretical potential energy in our analysis shown in Table 5 to get the final net energy. Whether 300 MW is a good estimate for the energy required to pump water from the Caspian Sea to Lake Urmia may be questioned, but are kept in this calculation for the sake of comparison with the results of Kelada [20].

3.3. Power density

When evaluating PRO potential, not only the total energy is important, but the power density measured as the number of watts produced per square meter membrane also matters. Power density can be calculated as the product of flux (J_w) and applied pressure (P_{appl}) on the draw solution.

$$P_d = J_w \cdot P_{appl} \tag{6}$$

Table 4
Water quality and discharge rate of the main discharging rivers to the Urmia Lake

Rivers	Concentration (mg/L)[a]							Discharge rate[b]
	Cl^-	SO_4^{2-}	Na^+	Mg^{2+}	Ca^{2+}	HCO_3^-	TDS	m^3/s
Shahr Chay	0.4	0.92	0.11	1	3.8	1.6	125	5.33
Barandooz Chay	0.1	0.22	0.22	1.4	3.4	2.45	162	8.3
Godar Chay	0.4	0.54	0.56	2.4	3.6	2.8	213	0.34
Mahabad Chay	0.35	1.34	0	1.6	4.6	2.85	229	6.5

[a]Water quality [40].
[b]Discharge rate [29].

Table 5
Energy estimated for the Caspian Sea and ZarrinehRud River discharging the Urmia Lake (results by Madsen's model, data from Kelada [20])

	River dicharge (m^3/s)	Lake salinity (mol/L)	NaCl (wt%)	kWh/m^3 river	Theoretical potential (MW)	Theoretical potential (MW)		Technical potential (MW)[a]	
						Lower limit	Upper limit	Lower limit	Upper limit
Urmia/Caspian Sea	100	5.47	26.6	3.15	1,134	454	567	154	267
Urmia/ZarrinehRud River	75	5.47	26.6	3.90	1,053	421	527		

[a]The technical potential energy was obtained by subtracting the energy required for the pumping to the high elevation (2,000 m above sea level ≈300 MW) [20].

Flux is dependent on the membrane permeability and the osmotic pressure difference as described by Eq. (7).

$$J_w = A\left(\Delta\pi - \Delta P\right) \tag{7}$$

During real operations, salt will accumulate on the membrane, giving rise to internal concentration polarization, and the water that permeates the membrane will dilute the saline drawn solution and lead to dilutive concentration polarization, which will lower the flux. These two effects can be accounted in the energy analysis by including the salt permeability constant, B, the membrane structural coefficient, S, the diffusion coefficient for salt, D, and the mass transfer coefficient for the drawing channel, k, in the equation for flux.

$$J_w = A\left(\frac{\pi_D \exp\left(-\frac{J_w}{k}\right) - \pi_F \exp\left(\frac{J_w S}{D}\right)}{1 + \frac{B}{J_w}\left(\exp\left(\frac{J_w S}{D}\right) - \exp\left(-\frac{J_w}{k}\right)\right)} - \Delta P\right) \tag{8}$$

To evaluate the potential power density for a PRO plant based on the ZarrinehRud River and water from the Caspian Sea as feedwaters, parameters for a standard membrane were assumed (A = 2.49 L/m²/h/bar, B = 0.39 L/m²/h, S = 564 µm, $D = 1.48 \times 10^{-9}$ m²/s and k = 99 L/m²/h) [43]. S is the structural parameter of the membrane, and can be considered of as a measure for the resistance of the membrane toward water flux. D is the diffusion coefficient of NaCl in water.

In the evaluation, a counter current setup is assumed, with draw inlet coinciding with feed inlet. It is presumed that the membrane module is designed so that all parts of the membrane are equally effective, with no dead zones. The same data as used for the total energy evaluation were used in this calculation. For all scenarios, a ratio of 1:1 for inlet draw volume and permeate volume was assumed while a slightly higher feed flow to allow for flushing of the salts in the remaining feedwater was assumed (feed to draw flow rate ratio = 1.2:1). To account for the higher salinity of the Caspian Sea water a higher flow of feedwater is necessary for this scenario (feed to draw flow rate ratio = 2:1). The ratio of feed and draw flow rate is one of the most important parameters in a PRO system. If a larger amount of feedwater is used, feed will be less concentrated, which will reduce concentration polarization and risk of fouling and scaling on the feed side of the membrane, which may increase power density. At the same time, the draw will become more diluted, which will lower the average osmotic gradient across the membrane leading to a reduced power density. If draw flow rate is increased relative to feed flow rate, the draw will become less diluted giving a larger average osmotic gradient and hereby a larger power density. However, more energy will be required for pumping draw water, which may negatively affect the overall energy production. Fig. 3 illustrates a graphical diagram

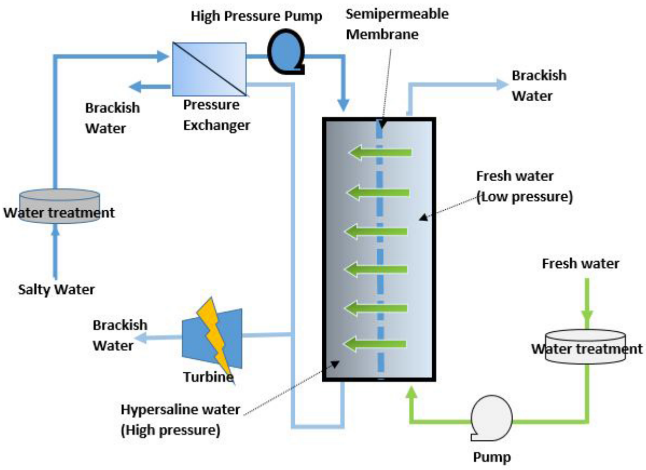

Fig. 3. Schematic diagram of a typical PRO power plant with counter current flow at steady-state condition.

Table 6
Average power density estimated for mixing water of ZarrinehRud River/Caspian Sea and Urmia Lake

Year	Inlet flow of lake water (m³/s)	Inlet flow of feedwater (m³/s)	Mixing ratio	Permeate volume (m³/s)	Salinity: Lake water inlet (mol/L)	Salinity: Feedwater outlet (mmol/L)	Salinity: Lake water outlet (mol/L)	Salinity: Feedwater inlet (mmol/L)	Operating pressure (bar)	Average power density (W/m²)
Data from Emdadi et al. [15]										
1994	1	1.2	0.55	1	1.69	3.42	0.81	0.48	19	15
1995	1	1.2	0.55	1	2.84	4.79	1.31	0.58	33	29
2000	1	1.2	0.55	1	5.20	4.28	2.27	0.40	50	53
2001	1	1.2	0.55	1	5.00	5.05	2.20	0.48	50	52
2003	1	1.2	0.55	1	4.96	4.62	2.28	0.44	50	51
2008	1	1.2	0.55	1	5.82	9.75	2.51	0.83	50	54
Data from Kelada [20]										
ZarrinehRud River	1	1.2	0.55	1	5.47	5.90	2.37	0.54	50	54
Caspian Sea	1	2	0.67	1	5.47	448	2.38	205	50	22

of a typical PRO power plant with counter current flow at steady-state condition.

The calculations were made by first determining the concentrations at inlet and outlet and then using these to produce curves of power density as a function of the applied pressure. These curves were used to determine the operating pressure, which was taken as the applied pressure that maximized power density at the draw outlet of the membrane (the point with lowest osmotic driving force). 50 bar was chosen as a maximum operating pressure since this is the highest pressure at which stable PRO has been reported in the literature [11].

In Table 6, the power density is reported as the average value of the inlet and outlet of the membrane module. This assumes that the power density will vary linearly through the module, which may not be true. Feed concentration will increase, while draw is diluted, and the change in osmotic pressure may not be equal for the two solutions resulting in an osmotic gradient that varies with the axial direction of the membrane. More elaborate methods that accounts for this variation have been reported [44,45], and the general finding here is that accounting for axial variation in the osmotic gradient will tend to give lower power densities than when a linear variation is assumed. However, the power densities calculated at the inlet and outlet will be accurate, not considering practical issues such as fouling and scaling. The lowest power density will be found at the draw outlet, and can be seen as the minimum power density that can be obtained with the membrane module, with the true value being somewhere between this and the power density at the draw inlet. The results show that power density increases with draw salinity as expected, and that power density higher than 5 W/m^2 could be obtained even when Lake Urmia was most diluted in the 90 s. A power density of 5 W/m^2 is typically reported as the value that must be exceeded to make PRO cost-effective [46]. The results also show that a scheme based on water from the Caspian Sea could be possible. Even though the higher salinity of the Caspian Sea compared with the ZarrinehRud River lowers the power density from 54 to 22 W/m^2, the value is still significantly higher than the 5 W/m^2.

4. Economic assessment

The costs of operation and maintenance in an SGE power plant are the most significant expenses for economic evaluation [13,47]. However, these costs depend on the membrane properties as a major component of the capital cost, particularly in a long-term operation [14,15,48,49]. The membrane is a fundamental element in the design of any SGE power plants [14,50]. For example, in a PRO process a membrane with higher water permeability, lower solute permeability and a low susceptibility to fouling can have a better performance [14,51]. Therefore, the economic feasibility of a PRO power plant can be estimated as the ratio of a PRO revenue over membrane area per year as it is described in Eq. (9) [6].

$$\frac{\text{Revenue}}{\text{Membrane area} \times \text{Year}} = \text{Power density} \times \text{Year} \tag{9}$$

To evaluate revenue, the power densities determined in section 3.3 for the ZarinehRud River and the Caspian Sea were used. In Eq. (8), the membrane revenue has a linear function with a retail price of electricity. The membrane revenue with the application of three membrane lifetime (1, 5 and 10) for the average power density of the ZarrinehRud (54 W/m^2) described in Fig. 4. It can be clearly seen a membrane with a higher lifetime (10 years or greater) will increase the revenue.

Since 2000, the PRO technologies have been significantly advancing. This development leads to a significant drop in the unit price of membranes (USD/m^2) [14]. For example, researchers anticipated the average cost of membrane per m^2 by \$4 drop reaches to \$2/m^2 in few years. Assuming a new membrane market for PRO production is emerging, and the average retail price of electricity has not been affected by the economic inflation; the lifetime of a membrane will play a major role in sensitivity analysis of the membrane revenue. Correlation between the membrane lifetime and the revenue per surface area of the membrane for the average power

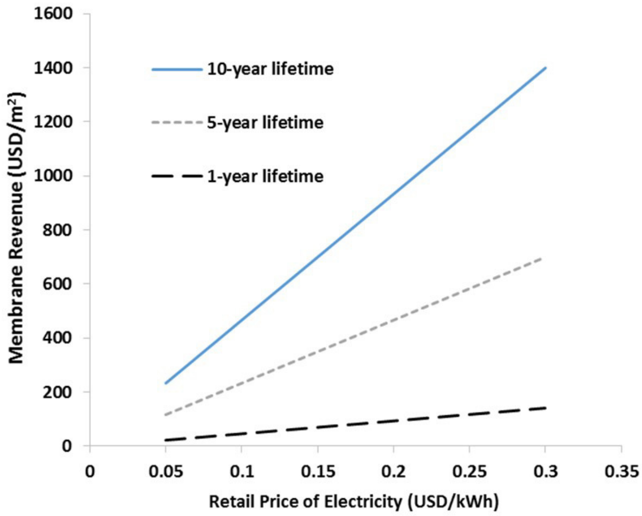

Fig. 4. Economic analysis for membrane revenue per surface area of the membrane as a function of the average retail price of electricity and durability of a membrane (lifetime) for the ZarrinehRud River.

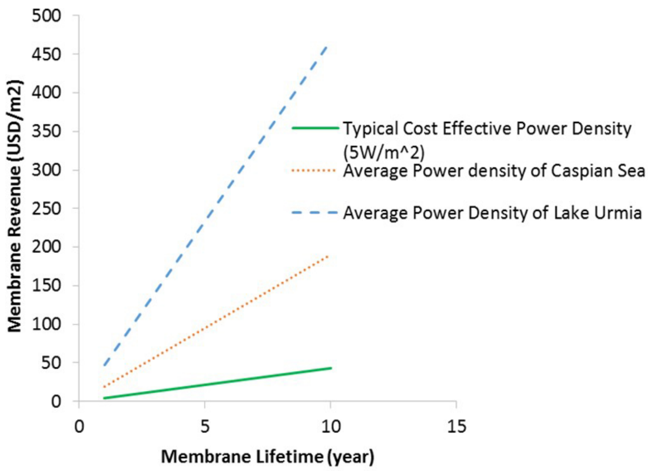

Fig. 5. Economic analysis for membrane revenue per surface area of the membrane as a function of membrane lifetime.

densities of the ZarinehRud River, Caspian Sea and a typical power density for a cost-effective plant (5 W/m^2) are presented in Fig. 5.

5. Outline and conclusion

Due to the hypersaline characteristic and existing freshwater rivers, Lake Urmia has a high potential for electricity production through mixing with freshwater [14] and transferring water from the Caspian Sea. In recent years, the water level of the lake has been declining due to dam construction and climate change [8,27]. As a consequence, the salinity has been increased which showed a positive effect on theoretical energy production. However, restoring the lake may increase the energy production due to low pressure on the membrane and less effects of fouling [52–54].

About 88% of the area of the lake has been declining in past decades. Currently, this lake is considered a highly endangered ecosystem [55]. Therefore, United Nations Development Programme (UNDP) established a restoration roadmap for Urmia Lake including: efficient management of water resource, support from national and international experts in design and saving plans, access to reliable data from research sources, promotion the exchange of ideas, technology and methods with international experts and extract of a valuable information [24].

The results of this paper ultimately accomplish this roadmap toward sustainable development and investigate the potential energy production of this lake through discharging rivers and possible water transfer from the Caspian Sea [27,31]. PRO energy production occurs in a natural system, which has a low environmental impact and zero GHG emissions [15,56,57]. Moreover, it can potentially supply the required energy for people who are living in the basin of the Lake and accomplish the energy policy of Iran (supply 2,526 MW from renewable energies) [58]. Rather than power generation, the freshwater rivers can still be functional for the irrigation of the local farmlands in this region.

The amount of energy in long-term production could have a return investment and create jobs for the local people. For instance, with developed membrane technologies and a better membrane market, a membrane with a power density of 22 w/m^2 can reduce the annual increase in electricity purchase price by at least 8% (i.e., 0.55 $/kWh) [59]. With this market, the feasibility of an economical construction of a PRO plant in the near future increases.

Due to developments in saline gradient technologies and economical supplies such as less expensive and cost-effective membranes [16], the possibility of investment and development of this renewable energy in Iran has been considerably raised [15,59]. However, the majority of decision makers in Iran have a poor understanding of natural resources and their potential values. The current situation of Lake Urmia is strong proof of this poor management over the last few decades. This article will hopefully help to raise the attention of the markets and decision makers for investment and protection of the lake.

Symbols

S — Membrane structural coefficient
M_{MX} — Molar mass of compound MX
K — Boltzmann's constant
D — Bulk diffusion coefficient
t_s — Thickness of the porous layer
τ — Tortuosity
ε — Porosity
B — Membrane solute permeability coefficient
C_D — Concentrations of the bulk draw
C_F — Concentrations of the bulk feed
R — Gas constant
T — Temperature, K
ΔG_{mix} — Gibbs free energy of mixing
φ_m — Mass-based mixing ratio
mi — Mass of solution i, kg
Pd — Power density, W/m^2
Q — Discharge, m^3/s
mo — Molal concentration, mol/kg solvent
αi — Activity of species i
b — B = 1.2 kg$^{1/2}$/mol$^{1/2}$
A_ϕ — Debye–Hückel parameters for the osmotic coefficient
Z_i — Ionic charge of species i
VXM — Molar volume of solution
x_i — Mole fraction
γ_i — Activity coefficients of each of the species present in the solution
φA — Ratio of the moles in solution A
φB — Ratio of the moles in solution B
I — Ionic strength
J_w — Flux of water through membrane
$\Delta\pi$ — Change of osmotic pressure
ΔP — Pressure compared with atmospheric conditions, Pa
C^{φ}_{MX} — Triplet ion-interaction parameter of Pitzer's equation for osmotic coefficient
V_{MX} — Molal volume of compound MX
$\gamma\pm$ — Mean ionic activity coefficient
α — Ionic strength dependence parameter in Pitzer's equation, α = 2 kg$^{1/2}$/mol$^{1/2}$
β^0_{MX} — β^1_{MX} Pairwise ion-interaction parameters in Pitzer's equations

References

[1] L. Sokka, T. Sinkko, A. Holma, K. Manninen, K. Pasanen, M. Rantala, P. Leskinen, Environmental impacts of the national renewable energy targets – a case study from Finland, Renew. Sustain. Energy Rev., 59 (2016) 1599–1610.

[2] Z.L. Cheng, X. Li, Y.D. Liu, T.-S. Chung, Robust outer-selective thin-film composite polyethersulfone hollow fiber membranes with low reverse salt flux for renewable salinity-gradient energy generation, J. Membr. Sci., 506 (2016) 119–129.

[3] I.L. Alsvik, M.-B. Hägg, Pressure retarded osmosis and forward osmosis membranes: materials and methods, Polymers, 5 (2013) 303–327.

[4] D. Attarde, M. Jain, S.K. Gupta, Modeling of a forward osmosis and a pressure-retarded osmosis spiral wound module using the Spiegler-Kedem model and experimental validation, Sep. Purif. Technol., 164 (2016) 182–197.

[5] N.Y. Yip, M. Elimelech, Performance limiting effects in power generation from salinity gradients by pressure retarded osmosis, Environ. Sci. Technol., 45 (2011) 10273–10282.

[6] A. Achilli, A.E. Childress, Pressure retarded osmosis: from the vision of Sidney Loeb to the first prototype installation — review, Desalination, 261 (2010) 205–211.

[7] W. He, Y. Wang, I.M. Mujtaba, M.H. Shaheed, An evaluation of membrane properties and process characteristics of a scaled-up pressure retarded osmosis (PRO) process, Desalination, 378 (2016) 1–13.

[8] E. Hassanzadeh, M. Zarghami, Y. Hassanzadeh, Determining the main factors in declining the Urmia Lake level by using system dynamics modeling, Water Resour. Manage., 26 (2012) 129–145.

[9] C.F. Wan, T.-S. Chung, Energy recovery by pressure retarded osmosis (PRO) in SWRO–PRO integrated processes, Appl. Energy, 162 (2016) 687–698.

[10] G. Han, S. Zhang, X. Li, T.-S. Chung, Progress in pressure retarded osmosis (PRO) membranes for osmotic power generation, Prog. Polym. Sci., 51 (2015) 1–27.

[11] H.T. Madsen, S.S. Nissen, E.G. Søgaard, Theoretical framework for energy analysis of hypersaline pressure retarded osmosis, Chem. Eng. Sci., 139 (2016) 211–220.

[12] N.Y. Yip, M. Elimelech, Thermodynamic and energy efficiency analysis of power generation from natural salinity gradients by pressure retarded osmosis, Environ. Sci. Technol., 46 (2012) 5230–5239.

[13] J.W. Post, J. Veerman, H.V.M. Hamelers, G.J.W. Euverink, S.J. Metz, K. Nymeijer, C.J.N. Buisman, Salinity-gradient power: evaluation of pressure-retarded osmosis and reverse electrodialysis, J. Membr. Sci., 288 (2007) 218–230.

[14] F. Helfer, C. Lemckert, Y.G. Anissimov, Osmotic power with pressure retarded osmosis: theory, performance and trends – a review, J. Membr. Sci., 453 (2014) 337–358.

[15] A. Emdadi, P. Gikas, M. Farazaki, Y. Emami, Salinity gradient energy potential at the hyper saline Urmia Lake–ZarrinehRud River system in Iran, Renew. Energy, 86 (2016) 154–162.

[16] F. Zabihian, A.S. Fung, Review of marine renewable energies: case study of Iran, Renew. Sustain. Energy Rev., 15 (2011) 2461–2474.

[17] A. Karbassi, G.N. Bidhendi, A. Pejman, M.E. Bidhendi, Environmental impacts of desalination on the ecology of Lake Urmia, J. Great Lakes Res., 36 (2010) 419–424.

[18] A. Eimanifar, F. Mohebbi, Urmia Lake (Northwest Iran): a brief review, Saline Syst., 3 (2007) 1–8.

[19] M. Kelada, Global Hyper Saline Power Generation Qattara Depression Potentials, Fourteenth International Middle East Power Systems Conference, Cairo, Egypt, 2010, pp. 19–21.

[20] M. Kelada, Global Potential of Hypersalinity Osmotic Power, MIK Technology, Houston, Texas, 2010, p. 12.

[21] C. Forgacs, Recent developments in the utilization of salinity power, Desalination, 40 (1982) 191–195.

[22] A. Yokozeki, Osmotic pressures studied using a simple equation-of-state and its applications, Appl. Energy, 83 (2006) 15–41.

[23] A.D. Wilson, F.F. Stewart, Deriving osmotic pressures of draw solutes used in osmotically driven membrane processes, J. Membr. Sci., 431 (2013) 205–211.

[24] W.A. Wurtsbaugh, B. Marden, P. Micklin, Lake Urmia Crisis and Roadmap for Ecological Restoration of Lake Urmia, United Nations Development Program, Iranian Department of Environment and Kalantari Commission, Tehran, Iran, 2014. Available at: http://works.bepress.com/wayne_wurtsbaugh/168/

[25] T. Ahmadzadeh Kokya, A. Pejman, E. Mahin Abdollahzadeh, B. Ahmadzadeh Kokya, M. Nazariha, Evaluation of salt effects on some thermodynamic properties of Urmia Lake water, Int. J. Environ. Res., 5 (2011) 343–348.

[26] M. Zeinoddini, M.A. Tofighi, F. Vafaee, Evaluation of dike-type causeway impacts on the flow and salinity regimes in Urmia Lake, Iran, J. Great Lakes Res., 35 (2009) 13–22.

[27] B. Pengra, The drying of Iran's Lake Urmia and its environmental consequences. GEAS UNEP, J. Environ. Develop., 2 (2012) 128–137.

[28] T. Talebi, E. Ramezani, M. Djamali, H.A.K. Lahijani, A. Naqinezhad, K. Alizadeh, V. Andrieu-Ponel, The Late-Holocene climate change, vegetation dynamics, lake-level changes and anthropogenic impacts in the Lake Urmia region, NW Iran, Quat. Int., 408 (2016) 40–51.

[29] M. Ghaheri, M. Baghal-Vayjooee, J. Naziri, Lake Urmia, Iran: a summary review, Int. J. Salt Lake Res., 8 (1999) 19–22.

[30] S. Alipour, Hydrogeochemistry of seasonal variation of Urmia Salt lake, Iran, Saline Syst., 2 (2006) 1448.

[31] UNDP, Lake Urmia and Its Basin: Characteristics, Current Situation, Drivers of Change, Management/Institutional Actions Undertaken and Planned, International Technical Round Table Towards a Solution for Iran's Drying Wetlands, UN Development Programme, 2014.

[32] H. Chitchian, Lake Urmia needs at least 10 years to revive, Mehr News Agency, 2015. Available at: http://en.mehrnews.com/news/108856/

[33] K. Kelts, M. Shahrabi, Holocene sedimentology of hypersaline Lake Urmia, Northwestern Iran, Palaeogeogr. Palaeoclimatol. Plaeoecol., 54 (1986) 105–130.

[34] A.G. Pervov, A.P. Andrianov, R.V. Efremov, A.V. Desyatov, A.E. Baranov, A new solution for the Caspian Sea desalination: low-pressure membranes, Desalination, 157 (2003) 377–384.

[35] H. Ghadiri, I. Dordipour, M. Bybordi, M. Malakouti, Potential use of Caspian Sea water for supplementary irrigation in Northern Iran, Agric. Water Manage., 79 (2006) 209–224.

[36] M.S. Ghiorso, I.S. Carmichael, M.L. Rivers, R.O. Sack, The Gibbs free energy of mixing of natural silicate liquids; an expanded regular solution approximation for the calculation of magmatic intensive variables, Contrib. Mineral. Petrol., 84 (1983) 107–145.

[37] K.S. Pitzer, J.C. Peiper, R. Busey, Thermodynamic properties of aqueous sodium chloride solutions, J. Phys. Chem. Ref. Data, 13 (1984) 1–102.

[38] F. Pérez-Villaseñor, S. Carro-Sánchez, G. Iglesias-Silva, Comparison among Pitzer-type models for the osmotic and activity coefficients of strong electrolyte solutions at 298.15 K, Ind. Eng. Chem. Res., 50 (2011) 10894–10901.

[39] T. Thorsen, T. Holt, The potential for power production from salinity gradients by pressure retarded osmosis, J. Membr. Sci., 335 (2009) 103–110.

[40] J.D. Khatuni, A. Mohammadi, A Report for Limnology and Paleolimnology of Urmia Lake, Geological Survey of Iran, 2011. Available at: http://www.geourmialake.com/ReportDetail.aspx?Cid=1

[41] O. Alvarez-Silva, C. Winter, A.F. Osorio, Salinity gradient energy at river mouths, Environ. Sci. Technol. Lett., 1 (2014) 410–415.

[42] N.Y. Yip, M. Elimelech, Comparison of energy efficiency and power density in pressure retarded osmosis and reverse electrodialysis, Environ. Sci. Technol., 48 (2014) 11002–11012.

[43] A.P. Straub, N.Y. Yip, M. Elimelech, Raising the bar: increased hydraulic pressure allows unprecedented high power densities in pressure-retarded osmosis, Environ. Sci. Technol. Lett., 1 (2013) 55–59.

[44] L.D. Banchik, M.H. Sharqawy, J.H. Lienhard, Limits of power production due to finite membrane area in pressure retarded osmosis, J. Membr. Sci., 468 (2014) 81–89.

[45] A.P. Straub, S. Lin, M. Elimelech, Module-scale analysis of pressure retarded osmosis: performance limitations and implications for full-scale operation, Environ. Sci. Technol., 48 (2014) 12435–12444.

[46] S.E. Skilhagen, Osmotic power—a new, renewable energy source, Desal. Wat. Treat., 15 (2010) 271–278.

[47] S.E. Skilhagen, J.E. Dugstad, R.J. Aaberg, Osmotic power — power production based on the osmotic pressure difference between waters with varying salt gradients, Desalination, 220 (2008) 476–482.

[48] Y. Chen, L. Setiawan, S. Chou, X. Hu, R. Wang, Identification of safe and stable operation conditions for pressure retarded osmosis with high performance hollow fiber membrane, J. Membr. Sci., 503 (2016) 90–100.

[49] J. Kim, M.J. Park, M. Park, H.K. Shon, S.-H. Kim, J.H. Kim, Influence of colloidal fouling on pressure retarded osmosis, Desalination, 389 (2016) 207–214.

[50] S.S. Hong, W. Ryoo, M.-S. Chun, G.-Y. Chung, Effects of membrane characteristics on performances of pressure retarded osmosis power system, Korean J. Chem. Eng., 32 (2015) 1249–1257.

[51] Q. She, X. Jin, C.Y. Tang, Osmotic power production from salinity gradient resource by pressure retarded osmosis: effects of operating conditions and reverse solute diffusion, J. Membr. Sci., 401–402 (2012) 262–273.

[52] X. Liu, L.-X. Foo, Y. Li, J.-Y. Lee, B. Cao, C.Y. Tang, Fabrication and characterization of nanocomposite pressure retarded osmosis (PRO) membranes with excellent anti-biofouling property and enhanced water permeability, Desalination, 389 (2016) 137–148.
[53] N.Y. Yip, M. Elimelech, Influence of natural organic matter fouling and osmotic backwash on pressure retarded osmosis energy production from natural salinity gradients, Environ. Sci. Technol., 47 (2013) 12607–12616.
[54] Q. She, Y.K.W. Wong, S. Zhao, C.Y. Tang, Organic fouling in pressure retarded osmosis: experiments, mechanisms and implications, J. Membr. Sci., 428 (2013) 181–189.
[55] A. AghaKouchak, H. Norouzi, K. Madani, A. Mirchi, M. Azarderakhsh, A. Nazemi, N. Nasrollahi, A. Farahmand, A. Mehran, E. Hasanzadeh, Aral Sea syndrome desiccates Lake Urmia: call for action, J. Great Lakes Res., 41 (2015) 307–311.
[56] J. Kuleszo, C. Kroeze, J. Post, B.M. Fekete, The potential of blue energy for reducing emissions of CO_2 and non-CO_2 greenhouse gases, J. Integr. Environ. Sci., 7 (2010) 89–96.
[57] S. Chou, R. Wang, L. Shi, Q. She, C. Tang, A.G. Fane, Thin-film composite hollow fiber membranes for pressure retarded osmosis (PRO) process with high power density, J. Membr. Sci., 389 (2012) 25–33.
[58] A. Kahrobaian, Renewable Energy in Islamic Republic of Iran: Policy Potential Energy Security Private Sector Application, Energy Security Seminar, Salzburg-Austria, 2010.
[59] A. Naghiloo, M. Abbaspour, B. Mohammadi-Ivatloo, K. Bakhtari, Modeling and design of a 25 MW osmotic power plant (PRO) on Bahmanshir River of Iran, Renew. Energy, 78 (2015) 51–59.